# 6.1 STRONG LINKS BETWEEN TELECONNECTIONS AND CANOPY CO2 EXCHANGE FOUND AT A PACIFIC OLD-GROWTH FOREST

Sonia Wharton*[1], Laura Chasmer[2], Matthias Falk[3] and Kyaw Tha Paw U[1]
[1]Atmospheric Science, University of California, Davis, California
[2] Dept. Geography, Queen's University, Kingston, Ontario
[3] CSTARS, University of California, Davis, California

## 1. ABSTRACT

Variability in three Pacific teleconnection patterns are examined to see if net carbon exchange at a low-elevation, old-growth forest is affected by climatic changes associated with these periodicities. Examined are the Pacific Decadal Oscillation (PDO), Pacific/North American Oscillation (PNA) and the El Niño-Southern Oscillation (ENSO). We use six years of eddy covariance $CO_2$, $H_2O$ and energy fluxes measured at the Wind River AmeriFlux site, Washington, USA.

The forest transitioned from an annual carbon sink (net ecosystem production (NEP) = + 207 g C $m^{-2}$ $year^{-1}$) to a source (NEP = - 100 g C $m^{-2}$ $year^{-1}$) during two dominant teleconnection patterns between 1999 and 2004. The carbon sink year (1999) occurred during a strong La Niña while the source year (2003) occurred during El Niño. When climate indices are in-phase, i.e. all are negative (cool) or positive (warm), the greatest anomalies in carbon flux and mechanistic variables (light use-, water use-efficiency) were observed. Annual averages were + 0.63 g C $m^{-2}$ $day^{-1}$ (- 0.27 g C $m^{-2}$ $day^{-1}$) for NEP, 3.1 mg C / g $H_2O$ (4.1 mg C / g $H_2O$) for WUE, and 1.7 g C $MJ^{-1}$ (2.1 g C $MJ^{-1}$) for LUE during in-phase cool (warm) years.

## 2. INTRODUCTION AND METHODS

*Site Description*

This research was carried out at the Wind River Canopy Crane AmeriFlux research station (latitude N 45°49'13.76'' and longitude W 121°57'06.88'', elevation 371 m above sea level) in southern Washington State (Fig. 1) during the years of 1999-2004. The 85 m tall canopy crane is located in a 500-hectare old-growth, conifer forest in the T.T. Munger Research Natural Area, a protected section of the Gifford Pinchot National Forest. The site has been unmanaged for centuries since originating from a natural fire disturbance. Despite the surrounding complex terrain of the western Cascade Mountains, the forest is located in a relatively flat valley (slope=3.5%). Maximum micrometeorological fetch reaches approximately 2 km within the homogeneous forest (Paw U *et al.* 2004).

* *Corresponding author address*: Sonia Wharton, Atmospheric Science, Univ. of California, Davis, One Shields Ave., Davis, CA 95616; email: swharton@ucdavis.edu. Webpage: http://atm.ucdavis.edu/~swharton

Shaw *et al.* (2004) provide a detailed site description for Wind River. Here described In brief, the two dominant tree species are Douglas-fir (*Pseudotsuga menziesii* (Mirbel) Franco) and western hemlock (*Tsuga heterophylla* (Raf.) Sarg). Trees within the site range in age from 0 to approximately 500 years old and reach maximum heights of 65 meters. Leaf area index (LAI) for the canopy has been estimated between 8.2 - 9.2 $m^2$ $m^{-2}$ (Parker *et al.* 2004) and total biomass is estimated at 619 g C $m^{-2}$ (Harmon *et al.* 2004). The local climate is characterized by very wet and mild (1 ºC, mean daily temperature) winters interspersed with a strong, seasonal summer drought (Shaw *et al.* 2004; Falk *et al.* 2005). At the site, annual mean air temperature is 8.7 $^{o}$C and total water-year (defined as October-September) precipitation is 2223 mm $year^{-1}$, of which on average only 322 mm falls from July through October.

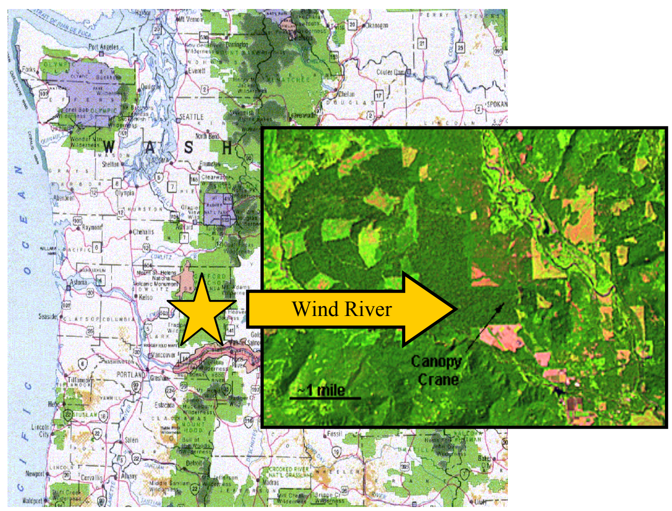


*Figure 1. Site location of the Wind River Canopy Crane.*

*Teleconnections and Regional Climate*

Terrestrial ecosystems along the western coast of North America are particularly prone to variations in climate via the eastward movement of weather patterns caused by equatorial and extratropical ocean-atmospheric oscillations (Mote *et al.* 2003). Atmospheric teleconnection patterns, particularly prevalent along the western coast of North America, include the Pacific Decadal Oscillation (PDO), the Pacific North American Oscillation (PNA) and the El Nino-Southern Oscillation (ENSO). ENSO typically transitions from a positive (warm) phase to a negative (cool) phase every 2 to 7 years in the equatorial Pacific Ocean. The impact of ENSO is felt in the extratropics through increased (El Niño) or decreased (La Niña) ocean temperature stratification and surface winds, and the associated strengthening (El Niño) or weakening (La Niña) of the Aleutian low. The PDO is described as the dominant mode of low-frequency (inter-decadal) variability in the North Pacific Ocean. A characteristic feature of the PDO is that sea surface temperatures (SST) normally remain consistently above or below the long-term average for two to three decades (Mantua & Hare 2002). The PNA is a second source of low frequency variability in the Northern Hemisphere extratropics and major phase shifts occur roughly every 10 years (Wallace & Gutzler 1981). Positive PNA phases are associated with an intensified Aleutian low pressure cell so that warmer air is transported northward along the western coast of North America. In the Pacific Northwest region of North America, positive phases of ENSO, PDO and PNA are associated with warmer and drier winters while negative phases bring cooler, wetter weather to the region.

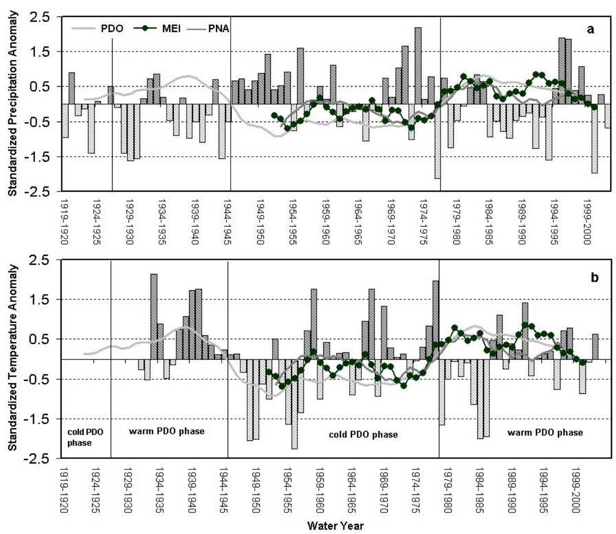


*Figure 2. Time series plot of standardized precipitation anomalies (a) and standardized temperature anomalies (b) from the Wind River region (1919-2004) in comparison to a 10-year smoothed PDO index, PNA index and 5-year smoothed multivariate ENSO index.*

Historical total precipitation (1919-1977) and mean air temperature (1931-1977) data were available from the Wind River Meteorological Station (45.48º N, 121.56º W, 351 meters a.s.l). Precipitation and air temperature data were available from 1977 through 2004 at the nearby Carson Fish Hatchery NOAA station (45.52º N, 121.58º W, 345.6 m a.s.l). The historical climate date record was used because it captures local temperature and precipitation anomalies during three complete PDO cycles between 1930 and 2000. We normalized the historical precipitation and air temperature data based on the long-term mean and standard deviation to produce standardized anomalies that could easily be compared to the climate indices (Fig. 2). Positive (negative) anomalies indicate wetter (drier) than normal or warmer (cooler) than normal conditions. This study uses the Multivariate ENSO Index (MEI) to describe El Niño and La Niña behavior.

Due to a high degree of autocorrelation between the three indices, we chose to concentrate on their additive effects during the flux measurement period and created a new climate index called a "composite climate index". The composite climate index (CCI) incorporates the PDO, PNA and MEI magnitudes into one single index by summing the three individual indices (Eqn.1).

$$CCI = PDO + PNA + MEI \qquad (1)$$

The annual composite index ranged in value from -1.6 (designated as a strong cool phase year) (1999) to +1.5 (designated as a strong warm phase year) (2003). The intermediate annual composite indices were grouped together as phase-neutral (2002-2002, 2004).

*Flux Tower Instrumentation*

Ecosystem carbon dioxide and water vapor fluxes were measured using the eddy covariance (EC) technique. The EC system consisted of a closed path Infrared Gas Analyzer (LI-6262, LiCor, Lincoln, Nebraska, USA) and an ultrasonic anemometer (Solent HS, Gill Instruments, Lymington, England, UK), both mounted at 70 m on an 87 m canopy crane. $CO_2$, $H_2O$, and turbulent velocities were measured at 10 Hz. Fluxes were calculated over a 30-minute averaging time using a horizontal rotation (vbar=0). Half-hourly $CO_2$ fluxes were further screened for outliers, gap-filled for missing values (using a running-mean approach, Reichstein *et al.* 2005), and ustar ($u_*$)-corrected at night using a friction velocity or $u_*$ critical value of 0.3 m $s^{-1}$ to replace carbon dioxide fluxes measured during stable nighttime turbulence conditions (Paw U *et al.* 2004; Falk 2005; Falk *et al.* 2008).

Meteorological data were also collected on a half-hourly basis. Soil moisture was measured with a time domain reflectometry (TDR) system (CSI TDR100, 6 CS610 probes) at integrated depths of 0-300 mm. Soil temperature (3 CS 107B probes) was measured at depths of 0, 15, 30 cm. Tower-mounted meteorological instrumentation included a 4-stream net radiometer (Kipp and Zonen CNR-1), up- and down-facing PAR sensors (LiCor 190SB), air temperature/humidity sensor (HMP35C) and barometric pressure sensor.

*Flux Calculations*

The flux data include a continuous, six year record starting in January 1999 and ending in December 2004, with all carbon dioxide exchange components integrated to daily, monthly and annual sums (Paw U *et al.* 2004; Falk *et al.* 2008). Daily net ecosystem production (NEP) (g C $m^{-2}$ $day^{-1}$) was calculated as the sum of half-hourly carbon dioxide fluxes:

$$NEP = -\sum(F_c + S_c) \qquad (2)$$

$F_c$ in Eqn (2) is the direct $CO_2$ flux measurement from the EC system. The carbon storage flux, $S_c$, was routinely computed for all half-hours using the mean carbon dioxide concentration. The effects of $S_c$ on monthly and annual NEP sums were found to be negligible because $S_c$ integrated to zero over monthly and annual time scales (Falk 2005). $F_c$ fluxes are negative when more carbon dioxide enters the plant canopy than is released to the atmosphere as a result of ecological processes. NEP, by definition, is positive when the net transport of carbon dioxide is downward into the canopy.

Daily ecosystem respiration (g C $m^{-2}$ $day^{-1}$), $R_{eco}$, was estimated based on an empirically derived, exponential fit ( $a \cdot e^{b \cdot T_{a2}}$ ) between half-hourly, nighttime $F_c$ data taken under sufficient turbulent mixing (when $u_*$ is > 0.3 m $s^{-1}$) and the 2 meter air temperature, $Ta_{02}$, and corrected for moisture limitations in the summer months (Falk *et al.* 2005):

$$R_{eco} = \sum((y_o + c * \exp(d * \theta_v)) * (a * \exp(b * Ta_{02})) \qquad (3)$$

The first term on the right hand side of Eqn (3) is a respiration attenuation function which is activated when soil water content ($\theta_v$) drops below 0.2 $m^3$ $m^{-3}$ and prevents the overestimation of ecosystem respiration on warm, dry summer days. All equation parameters (a-d, $y_o$) were empirically derived from nighttime, high turbulent flux data. For further details on the derivation of the respiration expression see Falk *et al.* (2005).

Daily NEP and $R_{eco}$ sums were used to estimate gross primary production (GPP) (g C $m^{-2}$ $day^{-1}$),

$$GPP = NEP + R_{eco} \qquad (4)$$

In Eqn (4), $R_{eco}$ and GPP are always positive fluxes and GPP is greater than $R_{eco}$ if NEP is positive. Monthly and annual NEP, $R_{eco}$, and GPP estimates were calculated from the sum of their corresponding daily fluxes. In this study we calculated annual NEP based on the Julian calendar year (January through December).

*Mechanistic Variables*

The influences of meteorological driving mechanisms on $CO_2$ and $H_2O$ fluxes are often manifested in efficiency parameters (e.g., WUE and LUE). Above canopy vapor pressure deficit (VPD), light use efficiency (LUE), water use efficiency (WUE), and fraction of intercepted photosynthetically active radiation (FIPAR) were derived using a combination of meteorological and eddy covariance instrumentation data.

VPD is important in canopy gas-atmosphere exchange because it drives stomatal conductance and can limit photosynthetic $CO_2$ uptake when VPD is high if soil moisture is limiting. Daily mean VPD was calculated using the half-hourly, 70 meter air temperature and relative humidity data during daylight periods only.

LUE is an estimate of the efficiency in which plants use light for carbon assimilation (Monteith 1972). In Eqn (5), we define daily LUE in terms of mass of carbon assimilated (g C) for every megajoule (MJ) of light intercepted by the canopy,

$$LUE = GPP / Q_i \qquad (5)$$

Where, GPP is gross primary productivity (g C $m^{-2}$ $day^{-1}$) and $Q_i$ is intercepted incoming PAR through the canopy (MJ $m^{-2}$ $day^{-1}$).

$$Q_i = Q_a (1 - e^{(-LAI * k)}) \qquad (6)$$

$Q_a$ is above canopy incident PAR (MJ $m^{-2}$ $day^{-1}$), LAI is 8.5 and the light extinction coefficient (k) was estimated using the Beer-Lambert law on a half-hourly basis in Eqn (6). In this study LUE was estimated from canopy intercepted PAR (IPAR) rather than using canopy absorbed PAR (APAR), which the latter includes ground-reflected PAR (Gower *et al.* 1999).

The fraction of PAR intercepted within the canopy (FIPAR) was estimated from incoming PAR measurements above ($Q_a$) and below ($Q_b$) the canopy at heights equal to 70 m and 2 m above the ground surface, respectively. Midday mean FIPAR was estimated for each day using the half-hour periods between 1000 and 1500, local standard time (LST).

$$FIPAR = 1 - (Q_b / Q_a) \qquad (7)$$

The WUE expression was modified to represent the total mass of carbon (mg C) assimilated for every gram of water lost by the ecosystem through evapotranspiration ($E_T$) (Eqn 8). The above canopy latent energy flux was used to calculate $E_T$ for all daylight half-hours when the latent energy flux was greater than zero (Berbigier *et al.* 2001). A midday mean WUE (mg C / g $H_2O$) was calculated using the half-hours 1000 and 1500 LST.

$$WUE = GPP / E_T \qquad (8)$$

*Fourier Analysis*

Spectral analysis was performed in this study using the Applied Statistical Time Series Analysis (ASTSA), a software package available from Shumway and Stoffer (1988). The power spectra were smoothed (smoothing = 5 data points per time series) to help resolve small spectral amplitude differences between frequencies. All power spectrum frequencies reported in this paper are significant above the 95$^{th}$ confidence interval.

## 3. RESULTS AND DISCUSSION

*Climatic fluctuations*

We found dominant spectral peaks at 3.5 and 5.3 years in the MEI record, 5.4 to 10.7 years in the PNA index and 5.7, 22.5 and 42.5 years in the PDO index, which are consistent with published values (Wallace & Gutzler 1981; Mantua *et al.* 1997; Wolter & Timlin 1998). Cool climate phases were most often associated with positive historical precipitation anomalies, while drier years occurred more frequently during warm phase events. The correlation between air temperature and climate phase was less significant, although cooler temperatures historically occurred more often during negative climate phases. The greatest temperature and precipitation anomalies occurred when the three climate indices were in-phase. During the flux measurement period (1999-2004), the positive phase year 2003 was on average 154 mm drier than normal, while the negative phase year (1999) was 748 mm above normal. Neutral-phase (2000-2002, 2004) precipitation amounts were close to the long-term average.

*Relationship between climate indices, local meteorology and carbon fluxes*

NEP was negatively correlated with temperature and positively correlated with precipitation, whereby higher precipitation amounts increase net carbon uptake and increased temperatures decrease net carbon uptake. Both relationships were not significant which suggests that the climate-carbon exchange interactions are complex and multivariate at Wind River.

Collectively, the PDO, PNA and MEI explained 90% of the observed variance in annual NEP, leaving just 10% unexplained. Nearly 80% of the annual NEP variance was explained by the PDO index alone. Fig. 3a shows a strong relationship ($R^2$ = 0.79, $P < 0.05$) between annual NEP and annual PDO, so that increased carbon uptake is associated with the cooler PDO phases. Cool climate phases bring cooler than normal air temperatures and higher than normal winter precipitation amounts. Fig. 3b shows that the relationship between monthly PDO and monthly NEP anomalies (deviations from the monthly, 1999-2004 mean) has more scatter ($R^2$ = 0.26) than the annual relationship but the correlation remains significant ($P <$ 0.005).

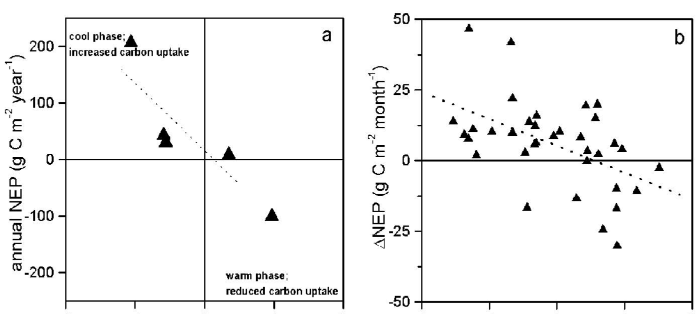


*Figure 3. Increased annual (a) and monthly (b) NEP is associated with negative annual PDO phases.*

Although the climate indices are not perfect predictors for annual ecosystem $CO_2$ sink/source strength, they do come close to estimating yearly NEP. The average standard error between measured annual NEP and climate index-predicted NEP was 0.58 g C $m^{-2}$ $yr^{-1}$ and is of the same order of magnitude as the uncertainty in the NEP measurements themselves. More importantly, the global climate indices were able to capture an observed NEP trend (Fig. 4). Since 1999, the climate indices have been transitioning to a more positive state whilst annual carbon uptake at the old-growth forest has declined over the last six years.

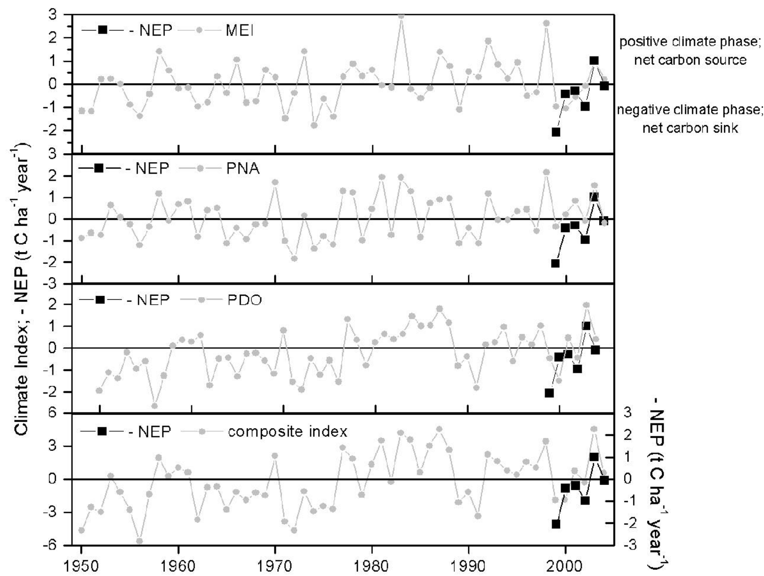


*Figure 4. Time series plot of winter MEI, PNA, PDO and composite index (1950-2004) values and annual NEP (1999-2004). The sign notation for NEP has been reversed so that a negative flux indicates net carbon uptake and a positive flux shows net carbon release by the forest ecosystem*

GPP anomalies were positively related to all three individual indices and are plotted against the composite climate index in Fig. 5 on both annual ($R^2$ = 0.83, $P <$ 0.05) and monthly time scales ($R^2$ = 0.33, $P < 0.0001$).

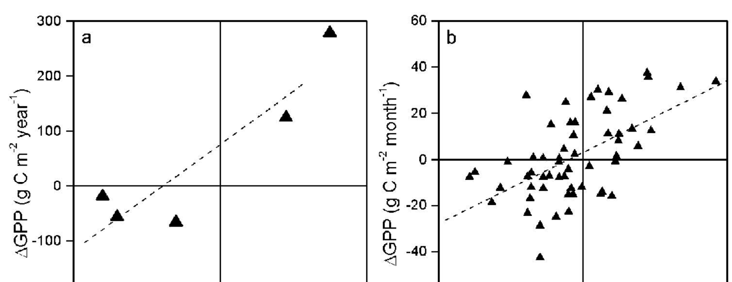


*Figure 5. Although increased carbon uptake (NEP) was associated with cool climate phases (Fig. 3), GPP was highest during warm phases (shown here).*

Ecosystem respiration anomalies were also positively correlated with the climate indices on annual

($R^2$ = 0.90, P < 0.05) and monthly time scales ($R^2$ = 0.38, P < 0.0001) (Fig. 6).

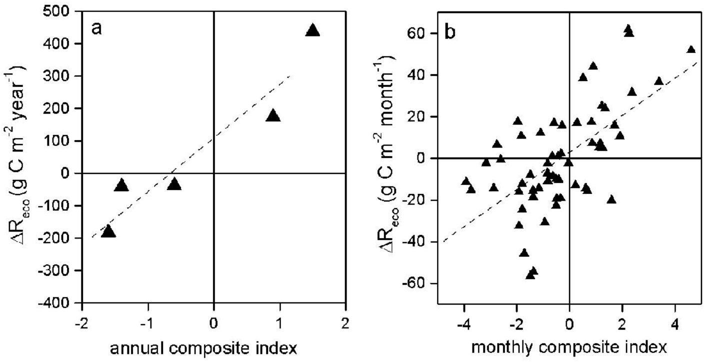


*Figure 6. Increased (decreased) respiration was associated with warmer (cooler) climate phases*

*Mechanistic anomalies*

Water-use efficiency was significantly lower in 1999 than during any other year (P < 0.0001). Mean (± one standard deviation) annual WUE was 3.1 ± 1.4 mg C / g $H_2O$ in 1999, 4.1 ± 1.5 mg C / g $H_2O$ in 2003, and 4.2 ± 1.5 mg C / g $H_2O$ during neutral phase years.

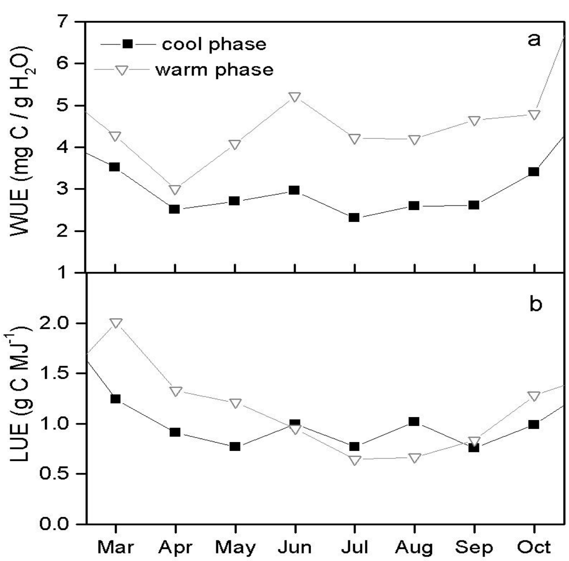


Figure 7. Monthly average midday WUE and LUE values in 1999 (cool phase) and 2003 (warm phase).

ANOVA single factor analysis revealed that annual light-use efficiency (LUE) was significantly higher in 2003 than during any other year (P < 0.05 against 1999 and P < 0.0001 against 2000-2002, 2004). The old-growth forest canopy was most efficient at using light for photosynthesis during warm-phase spring months (Fig. 7). During the 2003 early growing season, higher temperatures appear to increase LUE in the old-growth canopy. However, 2003 LUE was limited in the dry, warm summer by high VPD levels. Summer-time LUE was highest in 1999 and lower levels of ecosystem moisture-stress were suggested by low WUE efficiency ratios (Fig. 7) and below average VPD (not shown).

## 4. DISCUSSION

We found that the PDO, PNA and ENSO global climate indices together explained 90% of variance in annual NEP at the Wind River AmeriFlux site. Annual NEP ranged from + 217 g C m$^{-2}$ year$^{-1}$ (1999) to - 100 g C m$^{-2}$ year$^{-1}$ (2003) and coincided with in-phase cool and warm climate events, respectively. Flux measurements at a Vancouver Island Douglas-fir forest match the observed NEP trend at Wind River during the 1998-1999 ENSO transition. Morgenstern *et al.* (2004) report higher NEP (328 g C m$^{-2}$ year$^{-1}$) in 1999 than during the strong El Niño year of 1998 (296 g C m$^{-2}$ year$^{-1}$).

At Wind River, high annual NEP was associated with cool phases while high GPP fluxes were associated with warm climate phases. Hence, it is not an increase in GPP which is causing increased carbon uptake during cool climate phases. Instead, higher NEP values during cool phases resulted from decreased respiration rates which are likely driven by cooler temperatures (Falk *et al.* 2008).

WUE ratios at the old-growth forest differ from year to year depending on vegetation water demand. During periods of high precipitation and low VPD (1999), water stress is not chronic and trees can “afford” to keep their stomates open during midday hours throughout the summer to optimize photosynthesis. On the other hand, stomates regulate (limit) the amount of water lost through transpiration when VPD is high and soil moisture is limiting, producing higher WUE ratios during warm and dry conditions (2003).

LAI is relatively stable at a mature evergreen needleleaf forest like Wind River so any year-to-year difference in LUE cannot be attributed to significant leaf area change. During the cool phase year, GPP saturated at a lower light level (4 to 5 MJ day$^{-1}$) than during the warm phase year (6 to 7 MJ day$^{-1}$). 2003 also showed a higher saturation point for GPP which suggests that warmer spring-time temperatures were driving photosynthesis with no subsequent evidence of high VPD and soil water limitations, which would have had the effect of reducing GPP by inducing significant periods of stomatal closure. Higher LUE and a higher saturation point for GPP indicate that climate conditions were optimal for photosynthesis in the spring of 2003. The year was a warm phase year (all three indices are positive) and experienced a mean air temperature 1 ºC warmer than normal, but received 95% of normal precipitation.

## 5. CONCLUSION

Interannual variability of net carbon exchange and canopy processes for an old-growth forest in the Pacific Northwest can largely be explained by large-scale atmospheric circulation anomalies called teleconnection patterns. The largest ecosystem anomalies in NEP, GPP, $R_{eco}$, LUE and WUE occurred during in-phase climate events, i.e., when the composite climate index was at its highest positive or negative magnitude.

The results of the current study suggest that increases in the frequency or duration of negative-phase Northern Hemispheric, Pacific teleconnection patterns will increase annual carbon sequestration in some Pacific Northwest forests. However, stronger and more frequent positive phases will likely decrease net carbon uptake. Such strong, warm phase events can be considered to be "natural experiments" for testing hypotheses related to possible climate change scenarios.

## 6. ACKNOWLEDGEMENTS

This research was funded by the Western Regional Center (WESTGEC) of the National Institute for Global Environmental Change (NIGEC) through the U.S. Department of Energy (Cooperative Agreement No. DE-FC03-90ER61010). WRCCRF is operated under joint sponsorship of the University of Washington and the USDA Forest Service/PNW Station and we acknowledge both for significant support. Any opinions, findings, and conclusions or recommendations expressed herein are those of the authors and do not necessarily reflect the view of DOE.

## 7. REFERENCES

Berbigier P, Bonnefond J-M, Mellmann P (2001) CO2 and water vapour fluxes for 2 years above EuroFlux forest site. *Agricultural and Forest Meteorology*, **108**, 183-197.

Falk M (2005) *Carbon and energy exchange between an old-growth forest and the atmosphere*. PhD thesis, University of California, Davis, 216 pp.

Falk M, Paw U KT, Wharton S, Schroeder M (2005) Is soil respiration a major contributor to the carbon budget within a Pacific Northwest old-growth forest? *Agricultural and Forest* Meteorology, **135**, 269-283.

Falk M, Wharton S, Schroeder M, Ustin S, Paw U KT (2008) Flux partitioning in an old growth forest: seasonal and interannual dynamics. *Tree Physiology*, **28**, 509-520.

Gower ST, Kucharik CJ, Norman JM (1999) Direct and indirect estimation of leaf area index, fAPAR, and net primary production of terrestrial ecosystems. *Remote Sensing of the Environment*, **70**, 29-51.

Harmon ME, Bible K, Ryan MG, Shaw DC, Chen H, Klopatek J, Li X (2004) Production, respiration, and overall carbon balance in an old-growth *Pseudotsuga-tsuga* forest ecosystem. *Ecosystems*, **7**, 498-512.

Mantua NJ, Hare SR (2002) The Pacific decadal oscillation. *Journal of Oceanography*, **58**, 35-44.

Monteith JL (1977) Climate and the efficiency of crop production in Britain. *Philosophical Transactions of the Royal Society* B, **281**, 277–294.

Morgenstern K, Black TA, Humphreys ER *et al.* (2004) Sensitivity and uncertainty of the carbon balance of a Pacific Northwest Douglas-fir forest during an El Niño La Niña cycle. *Agricultural and Forest Meteorology*, **123**, 201-219.

Mote PW, Parson E, Hamlet AF *et al.* (2003) Preparing for climatic change: The water, salmon, and forests of the Pacific Northwest. *Climatic Change*, **61**, 45-88.

Parker GG, Harmon ME, Lefsky MA *et al.* (2004) Three-dimensional structure of an old-growth *Pseudotsuga-tsuga* canopy and its implications for radiation balance, microclimate, and gas exchange. *Ecosystems*, **7**, 440-453.

Paw U KT, Falk M, Suchanek TH *et al.* (2004) Carbon dioxide exchange between an old-growth forest and the atmosphere. *Ecosystems*, **7**, 513-524.

Reichstein M, Falge E, Baldocchi D *et al.* (2005) On the separation of net ecosystem exchange into assimilation and ecosystem respiration: review and improved algorithm. *Global Change Biology*, **11**, 1424-1439.

Shaw DC, Franklin JF, Bible K, Klopatek J, Freeman E, Greene S, Parker GG (2004) Ecological setting of the Wind River old-growth forest. *Ecosystems*, **7**, 427-439.

Shumway RH, Stoffer DS (1988) *Time Series Analysis and its Applications*, first edition, pp. 549, Springer Texts in Statistics, Springer-Verlag, New York.

Wallace JM, Gutzler DS (1981) Teleconnections in the geopotential height field during the Northern Hemispheric winter. *Monthly Weather Review*, **109**, 784-812.

Wolter K, Timlin MS (1998) Measuring the strength of ENSO events: How does 1997/1998 rank? *Weather*, **53**, 315-324.